Simultaneous Multi-User MIMO Communications and Multi-Target Tracking with Full Duplex Radios

Md Atiqul Islam[†], George C. Alexandropoulos[§], and Besma Smida[†]
[†]Department of Electrical and Computer Engineering, University of Illinois at Chicago, USA
[§]Department of Informatics and Telecommunications, National and Kapodistrian University of Athens, Greece
emails: {mislam23,smida}@uic.edu, alexandg@di.uoa.gr

Abstract—In this paper, we present an Integrated Sensing and Communications (ISAC) system enabled by in-band Full Duplex (FD) radios, where a massive Multiple-Input Multiple-Output (MIMO) base station equipped with hybrid Analog and Digital (A/D) beamformers is communicating with multiple DownLink (DL) users, and simultaneously estimates via the same signaling waveforms the Direction of Arrival (DoA) as well as the range of radar targets randomly distributed within its coverage area. Capitalizing on a recent reduced-complexity FD hybrid A/D beamforming architecture, we devise a joint radar target tracking and DL data transmission protocol. An optimization framework for the joint design of the massive A/D beamformers and the Self-Interference (SI) cancellation unit, with the dual objective of maximizing the radar tracking accuracy and DL communication performance, is presented. Our simulation results at millimeter wave frequencies using 5G NR wideband waveforms, showcase the accuracy of the radar target tracking performance of the proposed system, which simultaneously offers increased sum rate compared with benchmark schemes.

Index Terms—Full duplex, integrated communications and sensing, radar tracking, millimeter wave, massive MIMO.

I. INTRODUCTION

Integrated Sensing and Communications (ISAC) is emerging as a key feature of the next-generation wireless networks, where sensing and communication signaling operations are unified in a single system to considerably improve spectral and energy efficiencies while reducing both hardware and signaling costs [1]–[5]. In addition to its implementation in cellular networks, ISAC systems have recently been considered for a wide variety of applications, e.g., Wi-Fi networks [1], Unmanned Aerial Vehicle (UAV) networks [6], military communications [3], and localization for Vehicular networks (V2X) [7]. As a key enabler for ISAC applications, Full Duplex (FD) massive Multiple-Input Multiple-Output (MIMO) radios have the potential to be employed for the simultaneous DownLink (DL) transmission and UpLink (UL) reception capability within the entire frequency band [8]–[11]. FD multi-user massive MIMO systems in conjunction with fifth Generation (5G) millimeter Wave (mmWave) wideband waveforms can provide high-resolution radar target detection and tracking while ensuring high capacity communication links to DL users.

The principal bottleneck of the FD ISAC systems is the Self-Interference (SI) signal induced from the Transmitter (TX) to the Receiver (RX) at the massive MIMO FD Base Station (BS) node due to FD operation. Recently in [9], [11]–[13], a combination of propagation domain isolation, analog domain suppression, and digital SI cancellation techniques has been employed to achieve the required SI suppression for the mmWave FD massive MIMO transceivers. Hybrid Analog and Digital (A/D) BeamForming (HBF) is an attractive configuration for FD massive MIMO systems since it utilizes a small number of Radio Frequency (RF) chains connected to large-scale antenna arrays via phase shifters to reduce hardware cost. Appropriate A/D beamforming in the FD HBF system can reduce the impact of SI in the FD RX chains. Thus, a reduced complexity A/D SI cancellation solution can be formulated for FD massive MIMO systems with hybrid beamforming [9], [13].

Recently, single-antenna FD systems employing joint radar communication and sensing were introduced, where both communication and radar waveforms were studied for sensing performance [14], [15]. FD ISAC operations with mmWave massive MIMO systems were proposed in [16], [17]. A multibeam approach with dedicated beams towards both a radar target and a DL user was considered in [16], whereas the authors in [17] provided an ISAC technique detecting the Direction of Arrival (DoA) of two radar targets, while only successfully estimating the range of one target. In [18], we proposed a reduced complexity single-user FD ISAC system with massive MIMO BS operating at mmWave frequencies capable of estimating both the DoA and range of multiple radar targets, while maximizing the DL rate. However, none of the previous works provide an FD ISAC massive MIMO system with radar target tracking protocols across multiple communication slots with simultaneous multi-user DL communication.

In this paper, we present a multi-user FD ISAC system including a protocol for multiple radar target DoA tracking and range estimation across several communication subframes. The considered ISAC system employs an FD massive MIMO BS node communicating with multiple DL users, and utilizes the reflected waveforms to detect and track the radar targets residing within the communication environment. We propose a joint design of the A/D beamformers and a reduced complexity SI cancellation for the FD ISAC system, which target at maximizing the multi-user DL communication rate and the precision of the radar target tracking. We perform an extensive waveform simulation with 5G wideband Orthogonal Frequency Division Multiplexing (OFDM) waveforms at mmWave frequencies, verifying the performance of the proposed multi-user FD ISAC system.
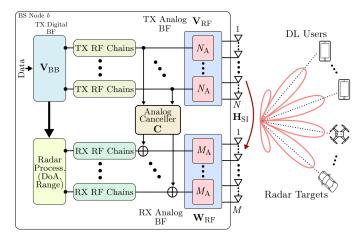
Fig. 1. The considered FD-enabled massive MIMO ISAC system, where the FD hybrid A/D beamforming BS communicates with DL users and simultaneously detects corresponding DoA and range of radar targets.

II. SYSTEM AND SIGNAL MODELS

We consider a multi-user FD massive MIMO ISAC system operating at mmWave frequencies, where an FD massive MIMO BS node is communicating with U RX user nodes in the DL direction, as depicted in Fig. 1. The DL signals are reflected by the multiple radar targets distributed within the communication environment, which are received and processed at the RX of BS node for radar targets' parameter estimation enabling integrated sensing and communication.

The FD massive MIMO BS node b is comprised of N TX and M RX antennas, whereas each of the U users has L RX antennas. To reduce the hardware complexity in massive MIMO BS node, we consider a small number of TX/RX RF chains partially-connected to Uniform Linear Arrays (ULAs) of large number of antenna elements via analog phase shifters following a Hybrid BeamForming (HBF) structure. Therefore, in the BS node, each of the N_{RF} and M_{RF} TX/RX RF chains are connected to ULAs of N_A and M_A antenna elements, respectively. The configurations of the phase shifters are contained in analog beamformers $\mathbf{V}_{RF} = \text{diag}(\mathbf{v}_1, \ldots, \mathbf{v}_{N_{RF}}) \in \mathbb{C}^{N \times N_{RF}}$ and $\mathbf{W}_{RF} = \text{diag}(\mathbf{w}_1, \ldots, \mathbf{w}_{N_{RF}}) \in \mathbb{C}^{M \times M_{RF}}$, respectively. The elements of the TX/RX analog BFs are assumed to have constant magnitude and chosen from predefined beam codebooks, i.e., $\mathbf{v}_n \in \mathbb{F}_{TX} \forall n = 1, \ldots, N_{RF}$ and $\mathbf{w}_m \in \mathbb{F}_{RX} \forall m = 1, \ldots, M_{RF}$. The TX/RX beam codebooks consists of $\text{card}(\mathbb{F}_{TX})$ and $\text{card}(\mathbb{F}_{RX})$ distinct analog beams, respectively. The RX user nodes are considered to employ fully digital beamforming, since the number of the user antennas is typically much smaller than at the FD massive MIMO BS.

A. DL and Radar Reflected Signals

We assume a 5G NR subframe-based DL signaling operation for the considered multi-user FD massive MIMO ISAC system. In each subframe, the BS transmits mmWave 5G NR OFDM waveforms to the DL users comprising Q OFDM symbols with P active subcarriers and Δf subcarrier spacing. In addition to the DL communication, these OFDM symbols are reflected

by multiple radar targets and received at the BS RX, which is utilized for tracking targets across subframes.

To enable multi-user MIMO communication, each subcarrier of the DL waveform contains L parallel data streams for each of the U DL users such that $UL \leq N_{RF}$. In the BaseBand (BB), the uth user's unit frequency-domain symbol vector $\mathbf{s}_{p,q,u} \in \mathbb{C}^L$ at the pth subcarrier of qth OFDM symbol is precoded using digital beamforming matrix $\mathbf{V}_{BB,u} \in \mathbb{C}^{N_{RF} \times L} \forall u = 1, \ldots, U$. Furthermore, the precoded signals are processed by the analog BF and the transmitted frequency-domain symbol vector $\mathbf{x}_{p,q} \in \mathbb{C}^N$ at the antenna elements can be written as

$$\begin{aligned} \mathbf{x}_{p,q} &\triangleq \mathbf{V}_{RF}[\mathbf{V}_{BB,1}, \ldots \mathbf{V}_{BB,U}][\mathbf{s}_{p,q,1}^T, \ldots, \mathbf{s}_{p,q,U}^T]^T \\ &= \mathbf{V}_{RF}\mathbf{V}_{BB}\mathbf{s}_{p,q}, \end{aligned} \tag{1}$$

where $\mathbf{V}_{BB} \triangleq [\mathbf{V}_{BB,1}, \ldots \mathbf{V}_{BB,U}] \in \mathbb{C}^{N_{RF} \times UL}$ and $\mathbf{s}_{p,q} \triangleq [\mathbf{s}_{p,q,1}^T, \ldots, \mathbf{s}_{p,q,U}^T]^T \in \mathbb{C}^{UL}$. The DL transmission is power limited such that $\mathbb{E}\{\|\mathbf{V}_{RF}\mathbf{V}_{BB}\mathbf{s}_{p,q}\|^2\} \leq P_b$, where P_b represents the maximum transmission power at node b.

For the integrated sensing operation, we assume K radar targets/scatters randomly distributed within the communication/sensing environment. Each of the K targets is associated with a DoD/DoA[1] $\theta_k \in [-\pi\ \pi]$ and a range δ_k from the BS node corresponding to a respective delay $\tau_k \triangleq 2\delta_k/c$, where c represents the speed of light. These radar targets reflect the DL transmitted signal $\mathbf{x}_{p,q}$, which is received at the RX of the FD BS node b. The radar RX signal $\mathbf{y}_{p,q} \in \mathbb{C}^M$ comprising reflected and SI signals is expressed as

$$\begin{aligned} \mathbf{y}_{p,q} &\triangleq \sum_{k=1}^K \alpha_k e^{-j2\pi\tau_k p\Delta f} \mathbf{a}_M(\theta_k)\mathbf{a}_N^H(\theta_k)\mathbf{x}_{p,q} \\ &\quad + \mathbf{H}_{SI}\mathbf{x}_{p,q} + \mathbf{n}_{p,q}, \end{aligned} \tag{2}$$

where $\mathbf{n}_{p,q} \sim \mathcal{CN}(0, \sigma_b^2 \mathbf{I}_M)$ and $\alpha_k \in \mathbb{C}$ denote the receiver noise vector with covariance σ_b^2 and the reflection coefficient of the kth radar target, respectively. The propagation delay τ_k induces the phase shift $e^{-j2\pi\tau_k p\Delta f}$ across subcarriers [19]. Here, the ith element of the ULA response vector $\mathbf{a}_N(\theta) \in \mathbb{C}^N$ with N antenna elements and any DoA θ is expressed as

$$[\mathbf{a}_N(\theta)]_i \triangleq \frac{1}{\sqrt{N}} e^{-j\frac{2\pi}{\lambda}(i-1)d\sin(\theta)}, \tag{3}$$

where λ and d are the signal wavelength and the inter-antenna element distance, respectively. Here, $\mathbf{H}_{SI} \in \mathbb{C}^{M \times N}$ is the Line-of-Sight (LoS) SI channel path between the TX and RX antenna arryas of the BS node b, which can be modeled as

$$[\mathbf{H}_{SI}]_{(m,n)} \triangleq \frac{\rho}{r_{m,n}} e^{-j\frac{2\pi}{\lambda}r_{m,n}}, \tag{4}$$

where, ρ represents the power normalization constant such that $\mathbb{E}\{\|[\mathbf{H}_{SI}]_{(m,n)}\|_F^2\} = MN$. Here, $r_{m,n}$ denotes the distance between mth RX and nth TX antenna elements at the BS node,

---

[1]It is to be noted that direction of departure and arrival of radar targets are identical since we consider a monostatic radar setup assuming relatively far away targets and small TX-RX array separation.

which depends on the transmit and receive array geometry [20, eq. (9)].

The received signal at the node b RX is processed by the RX analog combiner $\mathbf{W}_{\mathrm{RF}}$, which is followed by analog and digital cancellation to suppress the LoS SI signal below the noise floor. In the RX BB of the BS, the frequency-domain radar reflected symbol vector $\widetilde{\mathbf{y}}_{p,q} \in \mathbb{C}^{M_{\mathrm{RF}}}$ can be expressed as

$$\widetilde{\mathbf{y}}_{p,q} \triangleq \mathbf{W}_{\mathrm{RF}}^{\mathrm{H}} \sum_{k=1}^{K} \alpha_k e^{-j2\pi\tau_k p\Delta f} \mathbf{a}_M(\theta_k) \mathbf{a}_N^{\mathrm{H}}(\theta_k)\mathbf{x}_{p,q}$$
$$+ (\widetilde{\mathbf{H}}_{\mathrm{SI}} + \mathbf{C} + \mathbf{D})\mathbf{V}_{\mathrm{BB}}\mathbf{s}_{p,q} + \mathbf{W}_{\mathrm{RF}}^{\mathrm{H}}\mathbf{n}_{p,q}, \quad (5)$$

where $\mathbf{C} \in \mathbb{C}^{M_{\mathrm{RF}} \times N_{\mathrm{RF}}}$ and $\mathbf{D} \in \mathbb{C}^{M_{\mathrm{RF}} \times N_{\mathrm{RF}}}$ represent the low complexity analog and digital SI cancellers, respectively. After the analog cancellation, the residual SI signal satisfy the RX RF saturation constraint, i.e., $\|[(\widetilde{\mathbf{H}}_{\mathrm{SI}}+\mathbf{C})\mathbf{V}_{\mathrm{BB}}]_{(m,:)}\|^2 \leq \rho_b, \forall m = 1, \ldots, M_{\mathrm{RF}}$, where ρ_b represents the saturation level of RX RF chains at the BS node b. It is to be noted that the low complexity analog canceller $\mathbf{C}$ suppressing the LoS SI components is designed following the similar structure in [9]. Here, $\widetilde{\mathbf{H}}_{\mathrm{SI}} \triangleq \mathbf{W}_{\mathrm{RF}}^{\mathrm{H}}\mathbf{H}_{\mathrm{SI}}\mathbf{V}_{\mathrm{RF}}$ represents the effective LoS SI channel after analog TX/RX beamforming.

For the multi-user DL communication, we assume U out of K scatterers contribute to the DL channels from the BS node b to the U users. For each scatter, $\theta_u, \forall u = 1, \ldots, U$ represents the DoD, while ϕ_u denotes the DoA at the user node. The received DL signal vector at the uth user $\mathbf{r}_{p,q,u} \in \mathbb{C}^L$ is expressed as

$$\mathbf{r}_{p,q,u} \triangleq \beta_u \mathbf{a}_L(\phi_u)\mathbf{a}_N^{\mathrm{H}}(\theta_u)\mathbf{x}_{p,q} + \mathbf{z}_{p,q,u}$$
$$= \mathbf{H}_{\mathrm{DL},u}\mathbf{x}_{p,q} + \mathbf{z}_{p,q,u}, \quad (6)$$

where $\beta_u \in \mathbb{C}$ and $\mathbf{z}_{p,q,u} \sim \mathcal{CN}(0, \sigma_u^2\mathbf{I}_L)$ represent reflection coefficient of uth scatter and the noise floor at RX node u with covariance σ_u^2, respectively. Here, $\mathbf{H}_{\mathrm{DL},u} \triangleq \beta_u \mathbf{a}_L(\phi_u)\mathbf{a}_N^{\mathrm{H}}(\theta_u)$ represents the DL channel from BS node to uth user.

III. FD-ENABLED MULTI-TARGET TRACKING

In this section, we present the proposed FD ISAC DL data transmission and multiple radar target estimation and tracking operation. We utilize the received reflected signals at the BS node RX for estimation and tracking.

A. Radar Targets/Scatterers Evolution

We assume a 5G NR subframe-based DL communication system, where each radio subframe of T_s duration contains Q OFDM symbols with P subcarriers. The radar targets' and communication scatters' parameters are considered to remain constant for one subframe, while the parameters of the successive subframes are temporarily correlated. For any consecutive $(i-1)$ and ith subframes, the evolution of radar DoA components is expressed similar to [21] as

$$\theta_k[i] \triangleq \theta_k[i-1] + \Delta\theta_k, \quad \forall k = 1, \ldots, K, \quad (7)$$

where $\Delta\theta_k$ depends on the velocity of the kth radar target and the subframe duration T_s. For simplicity, we assume that all
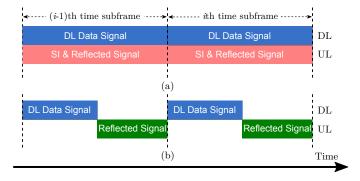

Fig. 2. (a) The Proposed FD-enabled ISAC scheme and (b) the conventional HD-based ISAC signaling in each time subframe.

the radar targets are moving with a constant velocity v in a circular direction from the BS, hence, $\Delta\theta_k \triangleq \arctan\left(\frac{vT_s}{\delta_k}\right)$. For brevity, the radar targets' complex-valued reflection coefficients α_k and DL channels complex path gains $\beta_u, \forall u$ are assumed to change randomly between consecutive time slots. In this paper, we propose to track only the radar targets' DoA components for each time subframe. The estimation of all complex path gains and reflection coefficients is left for future investigation.

B. ISAC Multi-Target Tracking Operation Protocol

The proposed FD ISAC protocol for DL data transmission and multiple radar target estimation and tracking is illustrated in Fig. 2(a), where the DL channel is dedicated for data transmission to the users while the UL is accessed at the BS node to receive the reflected signals from radar targets simultaneously. The procedures of FD ISAC transmission are described as follows:

1) At any $(i-1)$th time subframe, the DL signal reflected by the radar targets is received by the FD BS node b enabled by reduced complexity massive MIMO FD analog and digital canceller.

2) Utilizing the received signal after SI suppression, the DoAs of all K targets during $(i-1)$th time subframe $\widehat{\theta}_k[i-1], \forall k$ are estimated at the BS node b along with their range $\widehat{\delta}_k, \forall k$.

3) During the DL data transmission to U users at ith time subframe, the estimated DoAs $\widehat{\theta}_k[i-1]$ are used to choose appropriate digital beamformer $\mathbf{V}_{\mathrm{BB}}[i]$ and TX/RX phase shifter configurations $\mathbf{V}_{\mathrm{RF}}[i]$ and $\mathbf{W}_{\mathrm{RF}}[i]$ to assure maximized DL rate and satisfy RF saturation level constraint at the BS node b.

In Fig. 2(b), a conventional HD ISAC system is illustrated, where, contrary to the FD case, a portion of the subframe is dedicated for DL transmission while the rest is utilized for radar target detection.

C. Multiple Radar Targets' DoA Estimation

At the $(i-1)$th time subframe, we utilize the received reflected signal $\widetilde{\mathbf{y}}_{p,q}[i-1]$ to estimate the DoAs of K radar targets employing MUltiple SIgnal Classification (MUSIC) algorithm. First, we calculate the sample covariance matrix

across all subcarriers and OFDM symbols of $(i-1)$th subframe as

$$\widehat{\mathbf{R}}_b[i-1] \triangleq \frac{1}{PQ} \sum_{q=0}^{Q-1} \sum_{p=0}^{P-1} \widetilde{\mathbf{y}}_{p,q}[i-1]\widetilde{\mathbf{y}}_{p,q}^{\mathrm{H}}[i-1]. \quad (8)$$

Now, we perform the eigenvalue decomposition of the estimated sample covariance matrix $\widehat{\mathbf{R}}_b[i-1]$ as

$$\widehat{\mathbf{R}}_b[i-1] \triangleq \mathbf{U}\mathrm{diag}\{\eta_1, \eta_2, \ldots, \eta_{M_{\mathrm{RF}}}\}\mathbf{U}^{\mathrm{H}}, \quad (9)$$

where $\eta_1 \geq \eta_2 \geq \ldots \geq \eta_{M_{\mathrm{RF}}}$ are the eigenvalues in the descending order and $\mathbf{U} \in \mathbb{C}^{M_{\mathrm{RF}} \times M_{\mathrm{RF}}}$ represents the eigenvector matrix. The matrix $\mathbf{U}$ is partitioned into signal and noise subspace as $\mathbf{U} = [\mathbf{U}_s | \mathbf{U}_n]$, where $\mathbf{U}_n \in \mathbb{C}^{M_{\mathrm{RF}} \times M_{\mathrm{RF}} - K}$ and $\mathbf{U}_s \in \mathbb{C}^{M_{\mathrm{RF}} \times K}$ contains the noise and signal subspace eigenvectors. Now, we estimate the DoAs of K radar targets finding K peaks of the MUSIC spectrum formulated as

$$P_{\mathrm{MUSIC}}(\theta) \triangleq \frac{1}{\mathbf{a}_M^{\mathrm{H}}(\theta)\mathbf{W}_{\mathrm{RF}}[i-1]\mathbf{U}_n\mathbf{U}_n^{\mathrm{H}}\mathbf{W}_{\mathrm{RF}}^{\mathrm{H}}[i-1]\mathbf{a}_M(\theta)}. \quad (10)$$

The K peaks of $P_{\mathrm{MUSIC}}(\theta)$ correspond to the K estimated DoAs $\widehat{\theta}_k[i-1], \forall k$.

D. Multiple Radar Targets' Range Estimation

Now, we estimate the range of K radar targets at the $(i-1)$th subframe. As mentioned before, the range of radar targets $\delta_k, \forall k$ corresponds to propagation delay $\tau_k, \forall k$. Here, we obtain the estimated delay at $(i-1)$th subframe $\tau_k[i-1], \forall k$ from which respective range can be achieved. Utilizing the estimated DoAs $\widehat{\theta}_k[i-1]$ and the BB transmit signal vector $\mathbf{x}_{p,q}[i-1]$, we formulate a reference signal in the radar target direction as $\mathbf{g}_{p,q} \triangleq \mathbf{a}_M(\widehat{\theta}_k[i-1])\mathbf{a}_N^{\mathrm{H}}(\widehat{\theta}_k[i-1])\mathbf{x}_{p,q}[i-1]$. Now, we formulate a quotient across all RX antennas which includes the propagation delay impact in the direction of $\widehat{\theta}_k[i-1]$ as

$$z_{p,q} \triangleq \frac{1}{M} \sum_{m=1}^{M} \frac{[\mathbf{W}_{\mathrm{RF}}[i-1]\widetilde{\mathbf{y}}_{p,q}[i-1]]_m}{[\mathbf{g}_{p,q}[i-1]]_m}, \ \forall p, q, \quad (11)$$

The quotient $z_{p,q}$ is utilized to formulate a likelihood function as $A(n) \triangleq \sum_{q=0}^{Q-1} \sum_{p=0}^{P-1} z_{p,q}e^{j2\pi\frac{pn}{P}}$, where $n = 0, \ldots, P-1$ is the quantized delay parameters. Now, we find the best quantized delay that maximizes the likelihood function norm as follows

$$n^* \triangleq \arg\max_n \ |A(n)|^2. \quad (12)$$

Therefore, estimated delay of the kth target at $(i-1)$th subframe is expressed as $\widehat{\tau}_k[i-1] \triangleq \frac{n^*}{P\Delta f}$ and the range is formulated as $\widehat{\delta}_k[i-1] \triangleq \frac{\widehat{\tau}_k[i-1]c}{2}$. The DoA and delay estimation technique is utilized for any subframe to track the radar targets distributed within the communication environment.

Algorithm 1 Multi-user FD-Based ISAC Optimization

Input: $\widehat{\mathbf{H}}_{\mathrm{SI}}[i-1], \widehat{\mathbf{H}}_{\mathrm{DL},u}[i-1], N_C, \mathrm{P}_b$ and $\widehat{\theta}_k[i-1] \ \forall k$.
Output: $\mathbf{V}_{\mathrm{RF}}[i], \mathbf{V}_{\mathrm{BB}}[i], \mathbf{W}_{\mathrm{RF}}[i], \mathbf{C}[i]$, and $\mathbf{D}[i]$.

1: Set $\widehat{\mathbf{H}}_{\mathrm{R}}[i] = \sum_{k=1}^{K} \mathbf{a}_M(\widehat{\theta}_k[i-1])\mathbf{a}_N^{\mathrm{H}}(\widehat{\theta}_k[i-1])$.
2: Set $\mathbf{V}_{\mathrm{RF}}[i] \triangleq \arg\max_{\mathbf{v}_n \in \mathbb{F}_{\mathrm{TX}}, \forall n} \|\widehat{\mathbf{H}}_{\mathrm{R}}[i]\mathbf{V}\|^2$.
3: Set $\mathbf{W}_{\mathrm{RF}}[i] \triangleq \arg\max_{\mathbf{w}_m \in \mathbb{F}_{\mathrm{RX}}, \forall m} \frac{\|\mathbf{W}^{\mathrm{H}}\widehat{\mathbf{H}}_{\mathrm{R}}[i]\mathbf{V}_{\mathrm{RF}}[i]\|^2}{\|\mathbf{W}^{\mathrm{H}}\widehat{\mathbf{H}}_{\mathrm{SI}}[i-1]\mathbf{V}_{\mathrm{RF}}[i]\|^2}$.
4: Set $\widehat{\widetilde{\mathbf{H}}}_{\mathrm{SI}}[i] = \mathbf{W}_{\mathrm{RF}}^{\mathrm{H}}[i]\widehat{\mathbf{H}}_{\mathrm{SI}}[i-1]\mathbf{V}_{\mathrm{RF}}[i], \ \widehat{\widetilde{\mathbf{H}}}_{\mathrm{DL},u}[i] = \widehat{\mathbf{H}}_{\mathrm{DL},u}[i-1]\mathbf{V}_{\mathrm{RF}}[i], \forall u$.
5: Set $\mathbf{C}[i], \mathbf{D}[i]$ as in [18, Alg. 2], and $\mathbf{B}$ as the N_{RF} right-singular vectors of $(\widehat{\widetilde{\mathbf{H}}}_{\mathrm{SI}}[i]+\mathbf{C}[i])$.
6: **for** $\alpha = N_{\mathrm{RF}}, N_{\mathrm{RF}}-1, \ldots, 2$ **do**
7:   Set $\mathbf{F} = [\mathbf{B}]_{(:,N_{\mathrm{RF}}-\alpha+1:N_{\mathrm{RF}})}, \mathbf{H}_{\mathrm{eff},u} = \widehat{\widetilde{\mathbf{H}}}_{\mathrm{DL},u}[i]\mathbf{F}, \forall u$.
8:   Set $\bar{\mathbf{E}}_u \in \mathbb{C}^{N_{\mathrm{RF}} \times L}$ as the null space of effective DL channel with uth user removed $\bar{\mathbf{H}}_{\mathrm{eff},u} \triangleq [\mathbf{H}_{\mathrm{eff},1}^{\mathrm{T}}, \ldots, \mathbf{H}_{\mathrm{eff},u-1}^{\mathrm{T}}, \mathbf{H}_{\mathrm{eff},u+1}^{\mathrm{T}}, \ldots, \mathbf{H}_{\mathrm{eff},U}^{\mathrm{T}}]$.
9:   Set $\mathbf{E}_u$ as the right singular vectors of $\mathbf{H}_{\mathrm{eff},u}\bar{\mathbf{E}}_u$.
10:   Set $\mathbf{G}_u = \sqrt{\mathrm{P}_b/U}\bar{\mathbf{E}}_u\mathbf{E}_u$ as the optimum block-diagonalized precoder for uth user given P_b.
11:   Obtain digital precoder $\mathbf{G} = [\mathbf{G}_1, \ldots, \mathbf{G}_U]$ repeating steps 8-10 for all U users.
12:   **if** $\left\|[(\widehat{\widetilde{\mathbf{H}}}_{\mathrm{SI}}[i]+\mathbf{C}[i])\mathbf{F}\mathbf{G}]_{(m,:)}\right\|^2 \lessapprox \rho_b, \forall m$, **then**
13:     Output $\mathbf{V}_{\mathrm{BB}}[i] = \mathbf{F}\mathbf{G}$ and stop the algorithm.
14:   **else**
15:     Output $\mathbf{C}[i]$ does not meet the residual SI constraint.
16:   **end if**
17: **end for**

IV. PROPOSED OPTIMIZATION FRAMEWORK

In this section, we focus on the joint design of the A/D beamformers $\mathbf{V}_{\mathrm{BB}}[i], \mathbf{V}_{\mathrm{RF}}[i], \mathbf{W}_{\mathrm{RF}}[i]$ and SI cancellation matrices $\mathbf{C}[i], \mathbf{D}[i]$ at the ith subframe to optimize multi-user MIMO communication and multiple radar target tracking performance.

Our proposed FD ISAC optimization framework maximizes the Signal-to-Noise-Ratio (SNR) to the DL users as well as all the radar targets to optimize both tracking and DL communication. Utilizing the estimated DoAs of $(i-1)$th subframe $\widehat{\theta}_k[i-1], \forall k$, the SNR in all the radar targets' direction at the ith subframe can be expressed as,

$$\widehat{\Gamma}_{\mathrm{R}}[i] \triangleq \left\|\mathbf{W}_{\mathrm{RF}}^{\mathrm{H}}[i]\sum_{k=1}^{K}\mathbf{a}_M(\widehat{\theta}_k[i-1])\mathbf{a}_N^{\mathrm{H}}(\widehat{\theta}_k[i-1])\mathbf{V}_{\mathrm{RF}}[i]\right.$$
$$\left. \times \mathbf{V}_{\mathrm{BB}}[i]\right\|^2 \widehat{\Sigma}_b^{-1}[i], \quad (13)$$

where $\widehat{\Sigma}_b[i] = \|(\widehat{\widetilde{\mathbf{H}}}_{\mathrm{SI}}[i]+\mathbf{C}[i]+\mathbf{D}[i])\mathbf{V}_{\mathrm{BB}}[i]\|^2 + \|\mathbf{W}_{\mathrm{RF}}[i]\|^2\sigma_b^2$ represents the residual SI plus noise covariance. With the objective to maximize DL rate, we devise the sum of U DL users' SNR as

$$\widehat{\Gamma}_{\mathrm{DL}}[i] \triangleq \sum_{u=1}^{U} \left\|\widehat{\mathbf{H}}_{\mathrm{DL},u}[i-1]\mathbf{V}_{\mathrm{RF}}[i]\mathbf{V}_{\mathrm{BB}}[i]\right\|^2 \sigma_u^{-2}. \quad (14)$$

TABLE I
WAVEFORM AND SYSTEM LEVEL PARAMETERS

Parameter	Value	Parameter	Value
Carrier Frequency	28 GHz	Transmit Power	10:30 dBm
Bandwidth	100MHz	RX Noise Floor	-90 dBm
Subframe Duration, T_s	1ms	ADC Bits	14bits
OFDM Symbols, Q	14	PAPR	10 dB
Data Subcarriers, P	792	Dynamic Range	60 dB
Subcarrier Spacing, Δf	120 KHz	RF Saturation	-30 dBm

We formulate the optimization problem maximizing both SNR in the Radar target direction and DL users as

$$\mathcal{OP} : \max_{\substack{\mathbf{V}_{\mathrm{RF}}[i],\mathbf{V}_{\mathrm{BB}}[i],\mathbf{W}_{\mathrm{RF}}[i] \\ \mathbf{C}[i],\mathbf{D}[i]}} \widehat{\Gamma}_{\mathrm{R}}[i] + \widehat{\Gamma}_{\mathrm{DL}}[i]$$

$$\text{s.t. } \left\|[(\widehat{\widetilde{\mathbf{H}}}_{\mathrm{SI}}[i]+\mathbf{C}[i])\mathbf{V}_{\mathrm{BB}}[i]]_{(m,:)}\right\|^2 \leq \rho_b, \forall m = 1,\ldots, M_{\mathrm{RF}},$$

$$\mathbb{E}\{\|\mathbf{V}_{\mathrm{RF}}[i]\mathbf{V}_{\mathrm{BB}}[i]\|^2\} \leq \mathrm{P}_b, \quad (15)$$

$$\mathbf{w}_m[i] \in \mathbb{F}_{\mathrm{RX}}, \forall m \text{ and } \mathbf{v}_n[i] \in \mathbb{F}_{\mathrm{TX}}, \forall n = 1,\ldots, N_{\mathrm{RF}}$$

We employ an alternating optimization approach to solve this non-convex problem suboptimally. First, using the estimated DoAs $\widehat{\theta}_k[i-1] \ \forall k$ at any $(i-1)$th subframe, we find for the analog TX/RX BFs that maximizes the signal power toward all radar direction while minimizing the SI channel impact at the RX of BS node b. Utilizing the analog BFs, we follow a similar procedure as in [18] to find the $N_C \leq N_{\mathrm{RF}}M_{\mathrm{RF}}$ taps analog canceller. Finally, we design the multi-user digital precoder $\mathbf{V}_{\mathrm{BB}}$ using block diagonalization such that it maximizes the SNR of the DL users while minimizing the inter-user interference and suppressing the residual SI at node b. The proposed solution for (15) is summarized in Algorithm 1.

V. NUMERICAL RESULTS

In this section, we present the numerical evaluation of the proposed FD massive MIMO multi-user communication and multi-target tracking system through extensive waveform simulation.

A. Simulation Parameters

Following the FD massive MIMO architecture in Fig. 1, we consider a 128×128 FD massive MIMO BS node b with $N_{\mathrm{RF}} = M_{\mathrm{RF}} = 8$ TX/RX RF chains. Since the BS node employs a partially-connected beamforming structure, each TX/RX RF chain is connected to a ULA of $N_A = M_A = 16$ antenna elements via phase shifters. Both TX/RX phase shifter configurations (analog beams) are chosen from 5-bit Discrete Fourier Transform (DFT) codebooks. The multi-user MIMO communication is realized by $U = 2$ users, each with $L = 2$ RX antennas. We consider a mmWave communication of 28GHz frequency with 5G NR OFDM waveforms of 100MHz BandWidth (BW). Additional 5G NR waveform and system-level parameters are provided in Table. I. The DL channels from BS to the user are assumed to be clustered mmWave channels with 100dB pathloss. The LoS SI channel is simulated as (4) with 5mm TX-RX antenna array separation. The RX noise floors at all nodes are considered -90dBm, which results in -30dBm of RF saturation level at node b for effective dynamic range of 60dB considering 14-bit ADCs.
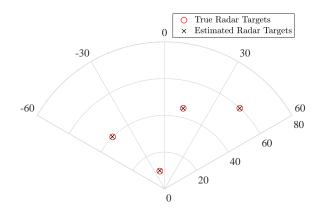

Fig. 3. DoA and range estimation performance of the proposed FD ISAC system for 4 radar targets with $N_{\mathrm{RF}} = M_{\mathrm{RF}} = 8, N_A = N_A = 16$ and DL transmit power of 30dBm.

Within the sensing/communication environment, $K = 4$ radar targets/scatters are considered out of which $U = 2$ contributes to the DL channel. Each K target is associated with a DoA $\theta_k \in [-60^{\circ} \quad 60^{\circ}], \forall k$ and a maximum range of 80m. We have simulated 20 radio subframes in each simulation run to evaluate the radar target estimation performance.

B. Multiple Radar Target Sensing Performance

In Fig. 3, we have illustrated the sensing performance of the proposed multi-user FD ISAC system with a 128×128 massive MIMO node transmitting DL signal with a transmit power of 30dBm. The estimated DoA and range of each radar target are depicted in the figure. It is evident that the proposed FD ISAC approach successfully estimates the DoA and range of all the $K = 4$ radar targets. The precise radar targets' DoA and range detection performance are due to the proposed target delay estimation associated with the high-resolution MUSIC approach.

C. Multi-Target Tracking Performance

In Fig. 4, we have plotted the Root Mean Square Error (RMSE) of the DoA tracking in degrees for all the radar targets across 20 5G NR radio subframes with different DoA evolution $\Delta\theta_k = [0.01^{\circ} \ 0.05^{\circ} \ 0.1^{\circ} \ 0.2^{\circ}]$ between consecutive subframes. For a range of 20m, an angle evolution of 0.2° corresponds to a velocity of 250km/h for radar targets. Therefore, the proposed FD ISAC approach is capable of tracking multiple radar targets moving at very high speed. For a moderate transmit power of 20dBm, the proposed approach provides less than 1° RMSE for most of the DoA evolution cases. However, the RMSE of DoA tracking for all different $\Delta\theta_k$ cases is around 0.25° for 30dBm transmit power exhibiting precise target tracking performance.

D. Multi-user DL Data Rate

The multi-user DL rate performance of the proposed FD ISAC system is depicted in Fig. 5 for different transmit powers, where the massive MIMO node b is communicating with 2 DL users. The proposed FD ISAC approach provides the DL rate within 1bps/Hz of the ideal FD rate up to 20dBm transmit
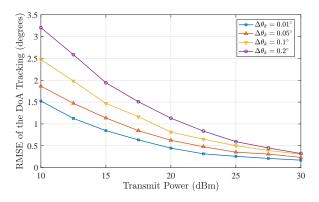
Fig. 4. DoA Tracking performance for 4 radar targets with $N_{\text{RF}} = M_{\text{RF}} = 8$, $N_{\text{A}} = N_{\text{A}} = 16$ and DL transmit power of 30dBm.

Fig. 5. Multi-user DL rate w.r.t. transmit power in dBm for the 128×128 massive MIMO FD BS communicating with $U = 2$ DL users.

power. However, with the increased impact of SI at high transmit powers, the FD ISAC system with 12.5% ($N = 8$) SI cancellation taps exhibits rate reduction compared to the ideal FD case. In contrast, the proposed approach with 25% taps provides comparable performance for all different transmit power values. Furthermore, the proposed FD ISAC system offers a superior multi-user DL rate compared to the ideal HD ISAC approach for all transmit power cases.

VI. CONCLUSION

In this paper, we presented a multi-user FD ISAC framework with an FD massive MIMO node simultaneously transmitting towards multiple DL users and estimating DoA as well as range of radar targets utilizing the reflected DL waveforms. We designed a radar target tracking and DL transmission protocol across multiple communication subframes. Utilizing a limited complexity analog SI cancellation for FD massive MIMO system, we presented a joint design of the A/D beamformer and analog SI cancellation that maximizes both radar target tracking and multi-user DL rate performance. Our performance results considering a mmWave channel model exhibited the high precision DoA and rage estimation of multiple radar targets while providing maximized multi-user DL rate.

ACKNOWLEDGMENTS

REFERENCES

[1] F. Liu, Y. Cui, C. Masouros, J. Xu, T. X. Han, Y. C. Eldar, and S. Buzzi, "Integrated sensing and communications: Towards dual-functional wireless networks for 6G and beyond," *IEEE J. Sel. Areas Commun.*, 2022.

[2] I. Alamzadeh *et al.*, "A reconfigurable intelligent surface with integrated sensing capability," *Scientific Reports*, vol. 11, no. 20737, pp. 1–10, Oct. 2021.

[3] F. Liu, C. Masouros, A. P. Petropulu, H. Griffiths, and L. Hanzo, "Joint radar and communication design: Applications, state-of-the-art, and the road ahead," *IEEE Trans. Commun.*, vol. 68, no. 6, pp. 3834–3862, Feb. 2020.

[4] G. C. Alexandropoulos *et al.*, "Hybrid reconfigurable intelligent metasurfaces: Enabling simultaneous tunable reflections and sensing for 6G wireless communications," *[online] https://arxiv.org/abs/2104.04690*, 2021.
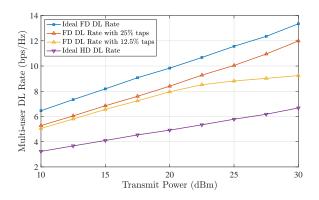
[5] K. V. Mishra, M. B. Shankar, V. Koivunen, B. Ottersten, and S. A. Vorobyov, "Toward millimeter-wave joint radar communications: A signal processing perspective," *IEEE Signal Process. Mag.*, vol. 36, no. 5, pp. 100–114, Sep. 2019.

[6] X. Wang, Z. Fei, J. A. Zhang, J. Huang, and J. Yuan, "Constrained utility maximization in dual-functional radar-communication multi-UAV networks," *IEEE Trans. Commun.*, vol. 69, no. 4, pp. 2660–2672, Dec. 2020.

[7] H. Wymeersch, G. Seco-Granados, G. Destino, D. Dardari, and F. Tufvesson, "5G mmWave positioning for vehicular networks," *IEEE Wireless Commun.*, vol. 24, no. 6, pp. 80–86, Dec. 2017.

[8] M. A. Islam *et al.*, "A unified beamforming and A/D self-interference cancellation design for full duplex MIMO radios," in *Proc. IEEE PIMRC*, Istanbul, Turkey, Sep. 2019.

[9] G. C. Alexandropoulos *et al.*, "Full duplex hybrid A/D beamforming with reduced complexity multi-tap analog cancellation," in *Proc. IEEE SPAWC*, Atlanta, USA, May 2020.

[10] M. A. Islam *et al.*, "Simultaneous data communication and channel estimation in multi-user full duplex MIMO systems," in *Proc. IEEE ASILOMAR*, Pacific Grove, USA, Nov. 2020.

[11] A. Sabharwal, P. Schniter, D. Guo, D. W. Bliss, S. Rangarajan, and R. Wichman, "In-band full-duplex wireless: Challenges and opportunities," *IEEE J. Sel. Areas Commun.*, vol. 32, no. 9, pp. 1637–1652, Sep. 2014.

[12] M. A. Islam *et al.*, "Direction-assisted beam management in full duplex millimeter wave massive MIMO systems," in *Proc. IEEE GLOBECOM*, Madrid, Spain, Dec. 2021.

[13] I. P. Roberts *et al.*, "Equipping millimeter-wave full-duplex with analog self-interference cancellation," in *Proc. IEEE ICC*, Ireland, Jun. 2020.

[14] C. B. Barneto *et al.*, "Full-duplex OFDM radar with LTE and 5G NR waveforms: Challenges, solutions, and measurements," *IEEE Trans. Microw. Theory Techn.*, vol. 67, no. 10, pp. 4042–4054, Aug. 2019.

[15] S. D. Liyanaarachchi *et al.*, "Optimized waveforms for 5G–6G communication with sensing: Theory, simulations and experiments," *IEEE Trans. Wireless Commun.*, Jun. 2021.

[16] C. B. Barneto, S. D. Liyanaarachchi, T. Riihonen, M. Heino, L. Anttila, and M. Valkama, "Beamforming and waveform optimization for OFDM-based joint communications and sensing at mm-waves," in *Proc. IEEE ASILOMAR*, Pacific Grove, USA, Nov. 2020, pp. 895–899.

[17] S. D. Liyanaarachchi *et al.*, "Joint multi-user communication and MIMO radar through full-duplex hybrid beamforming," in *IEEE Int. Symp. Joint Commun. & Sensing (JC&S)*, Feb. 2021, pp. 1–5.

[18] M. A. Islam *et al.*, "Integrated sensing and communication with millimeter wave full duplex hybrid beamforming," in *Proc. IEEE ICC*, Seoul, South Korea, May 2022.

[19] M. Braun, C. Sturm, and F. K. Jondral, "Maximum likelihood speed and distance estimation for OFDM radar," in *IEEE Radar Conf.*, May 2010, pp. 256–261.

[20] K. Satyanarayana *et al.*, "Hybrid beamforming design for full-duplex millimeter wave communication," *IEEE Trans. Veh. Technol.*, vol. 68, no. 2, pp. 1394–1404, Dec. 2018.

[21] V. Va *et al.*, "Beam tracking for mobile millimeter wave communication systems," in *Proc. IEEE GlobalSIP*, Dec. 2016, pp. 743–747.